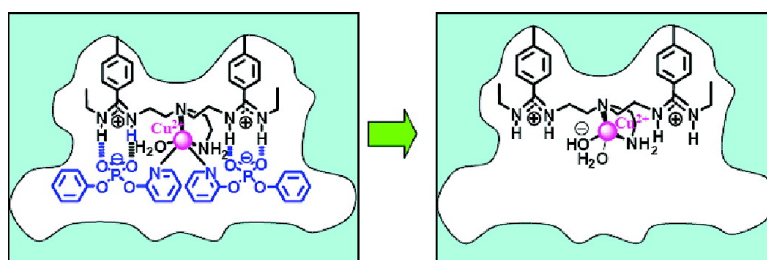


Functional Mimicry of Carboxypeptidase A by a Combination of Transition State Stabilization and a Defined Orientation of Catalytic Moieties in Molecularly Imprinted Polymers

Jun-qiu Liu, and Gu#nter Wulff

J. Am. Chem. Soc., **2008**, 130 (25), 8044-8054 • DOI: 10.1021/ja8012648 • Publication Date (Web): 30 May 2008

Downloaded from <http://pubs.acs.org> on February 8, 2009



More About This Article

Additional resources and features associated with this article are available within the HTML version:

- Supporting Information
- Access to high resolution figures
- Links to articles and content related to this article
- Copyright permission to reproduce figures and/or text from this article

[View the Full Text HTML](#)

Functional Mimicry of Carboxypeptidase A by a Combination of Transition State Stabilization and a Defined Orientation of Catalytic Moieties in Molecularly Imprinted Polymers

Jun-qiu Liu*[‡] and Günter Wulff*[†]

Institute of Organic and Macromolecular Chemistry, Heinrich Heine University, 40225 Düsseldorf, Germany and the State Key Laboratory of Supramolecular Structure and Materials, Jilin University, Changchun, 130012, P. R. China

Received February 20, 2008; E-mail: wulffg@uni-duesseldorf.de; junqiliu@jlu.edu.cn

Abstract: An artificial model for the natural enzyme carboxypeptidase A has been constructed by molecular imprinting in synthetic polymers. The tetrahedral transition state analogues (TSAs **4** and **5**) for the carbonate hydrolysis have been designed as templates to allow incorporation of the main catalytic elements, an amidinium group and a Zn²⁺ or Cu²⁺ center, in a defined orientation in the transition state imprinted active site. The complexation of the functional monomer and the template in presence of Cu²⁺ through stoichiometric noncovalent interaction was established on the basis of ¹H NMR studies and potentiometric titration. The Cu²⁺ center was introduced into the imprinted cavity during polymerization or by substitution of Zn²⁺ in Zn²⁺ imprinted polymers. The direct introduction displayed obvious advantages in promoting catalytic efficiency. With substrates exhibiting a very similar structure to the template, an extraordinarily high enhancement of the rate of catalyzed to uncatalyzed reaction ($k_{\text{cat}}/k_{\text{uncat}}$) of 10⁵-fold was observed. If two amidinium moieties are introduced in proximity to one Cu²⁺ center in the imprinted cavity by complexation of the functional monomer **3** with the template **5**, the imprinted catalysts exhibited even higher activities and efficiencies for the carbonate hydrolysis with $k_{\text{cat}}/k_{\text{uncat}}$ as high as 410 000. These are by far the highest values obtained for molecularly imprinted catalysts, and they are also considerably higher compared to catalytic antibodies. Our kinetic studies and competitive inhibition experiments with the TSA template showed a clear indication of a very efficient imprinting procedure. In addition, this demonstrates the important role of the transition state stabilization during the catalysis of this reaction.

1. Introduction

Natural enzymes catalyze reactions with high stereoselectivity and efficiency. To elucidate the catalytic nature of enzyme efficiency many practical and fundamental efforts have been made. Although the major evidence of the catalytic mode of operation were provided by biochemical and structural studies,¹ the design of synthetic catalysts as enzyme mimics has become an important aspect in understanding the molecular interactions involved in substrate recognition and catalysis.² In recent years, chemists showed an increasing interest in the design of highly selective catalysts, not only for providing more insight into the mechanisms of molecular recognition and catalysis in enzymes,

but also for practical applications in chemistry, biology, and medicine.²

Initial efforts in this regard have focused on the construction of small host molecules with defined cavities as well as carrying catalytic groups and cofactors.² Notable examples include synthetic model systems consisting of cyclodextrins^{2c,d} and macrocyclic amines^{2g} as well as other macrocyclic compounds.² More recently, promising success has been achieved in the design of macromolecular receptors capable of selectively binding and catalyzing defined substrates.^{3–5} Among them are catalytic antibodies,³ chemically modified naturally occurring enzymes and receptors,⁴ as well as synthetic polymers.^{5,2f} Using the concept of transition state stabilization known from enzyme catalysis, catalytically quite active antibodies have been raised against stable transition state analogues (TSAs) of the corre-

[†] Heinrich Heine University.

[‡] Jilin University.

- (1) (a) Wolfenden, R. *Science* **1983**, *222*, 1087–1093. (b) Warshel, A. *Proc. Natl. Acad. Sci. U.S.A.* **1984**, *81*, 444–448. (c) Benkovic, S. J.; Hammes-Schiffer, S. *Science* **2003**, *301*, 1196–1202. (d) Radkiewicz, J. L.; Brooks, C. L., III *J. Am. Chem. Soc.* **2000**, *122*, 225–231. (e) Kahn, K.; Bruce, T. C. *J. Am. Chem. Soc.* **2000**, *122*, 46–51.
- (2) (a) Kirby, A. *Angew. Chem., Int. Ed.* **1996**, *35*, 707–724. (b) Kirby, A. *Acc. Chem. Res.* **1997**, *30*, 290–296. (c) Breslow, R.; Dong, S. D. *Chem. Rev.* **1998**, *98*, 1997–2011. (d) Breslow, R.; Graff, A. *J. Am. Chem. Soc.* **1993**, *115*, 10988–10989. (e) Chin, J. *Acc. Chem. Res.* **1991**, *24*, 145–152. (f) Suh, J. *Acc. Chem. Res.* **2003**, *36*, 562–570. (g) Kimura, E. *Acc. Chem. Res.* **2001**, *34*, 171–179. (h) Motherwell, W. B.; Bingham, M. J.; Six, Y. *Tetrahedron* **2001**, *57*, 4663–4686. (i) Houk, K. N.; Leach, A. G.; Kim, S. P.; Zhang, X. *Angew. Chem.* **2003**, *115*, 5020–5046; *Angew. Chem., Int. Ed.* **2003**, *42*, 4872–4897.

- (3) (a) Lerner, R. A.; Benkovic, S. J.; Schultz, P. G. *Science* **1991**, *252*, 659–667. (b) Schultz, P. G.; Lerner, R. A. *Science* **1995**, *269*, 1835–1842. (c) Hilvert, D.; Hill, K. W.; Narel, K. D.; Auditor, M.-T. M. *J. Am. Chem. Soc.* **1989**, *111*, 9261–9262.
- (4) (a) Qi, D. F.; Tann, C. M.; Haring, D.; Distefano, M. D. *Chem. Rev.* **2001**, *101*, 3081–3111. (b) DeSantis, G.; Jones, J. B. *Curr. Opin. Biotechnol.* **1999**, *10*, 324–330. (c) Penning, T. M. *Chem. Rev.* **2001**, *101*, 3027–3046.
- (5) (a) For reviews, see: Wulff, G. *Chem. Rev.* **2002**, *101*, 1–27. (b) Ramström, O.; Mosbach, K. *Curr. Opin. Chem. Biol.* **1999**, *3*, 759–764. (c) Severin, K. In *Molecularly Imprinted Materials. Science and Technology*; Yan, M., Ramström, O., Eds.; Marcel Dekker: New York, 2005; pp 619–683.

sponding reaction.³ Similarly, molecularly imprinted polymers (MIPs) offer an excellent possibility to mimic the active site of natural enzymes since not only the shape of the transition state can be mimicked by imprinting but also, at the same time, suitable catalytically active groups and binding sites can be introduced into the active site in a predetermined orientation.⁵

In molecular imprinting a highly cross-linked copolymer is formed during polymerization around a template molecule. The monomer mixture contains functional monomers that can reversibly interact with the template through covalent or noncovalent interactions. The resultant complex is subsequently incorporated into a network polymer by copolymerization in the presence of an excess of a cross-linking monomer and a solvent acting as an inert porogen. After removal of the template from the macroporous polymer, an imprint containing functional groups in a certain orientation remains in the polymer. The shape of the formed imprint and the arrangement of the functional groups are complementary to the structure of the template.^{5,6} Such imprinted polymers show high selectivity in rebinding to their own template molecules. Molecularly imprinted polymers show antibody-like recognition characteristics and have meanwhile been prepared for a large number of compound classes. Their preparation has also become an efficient approach for the development of synthetic enzyme models with high selectivity. By analogy to the preparation of catalytic antibodies,³ numerous experiments have been undertaken to mimic enzyme behavior by imprinting with stable transition state analogues (TSAs) in reactions including dehydrofluorination, hydrolyses, Diels–Alder reactions, transaminase reactions, and others.^{7,8}

Although earlier attempts to mimic enzyme behavior using imprinted polymers showed only low or moderate catalytic efficiency,⁷ very promising results for catalyzed hydrolyses were obtained in recent years using MIP catalysts.^{8,9} It follows from these results that the ability for TSA binding alone is not sufficient to obtain a really high rate of acceleration; increasing the transition state binding by steric and electronic effects in combination with correctly incorporating and positioning the functional groups is essential for the construction of an effective enzyme model.^{2,9}

Previously, MIP-based catalysts with both TSA binding sites and appropriate catalytic groups have been prepared in our group

in order to emulate carboxypeptidase A-like activity.⁹ An unusually high catalytic activity for carbonate hydrolysis was obtained by imprinting with a stable transition state analogue template as well as introduction of an amidinium group and a Cu(II)^{9a} or Zn(II)^{9b} center into the active site in a defined orientation to each other.

Carboxypeptidase A (CPA, EC3.4.17.1) is a zinc-containing metalloprotease that has the function of removing the C-terminal amino acid residue from a peptide chain.¹⁰ As one of the most intensively studied enzymes, CPA has contributed enormously to the elucidation of the catalytic mechanism of other metalloenzymes and also served as a model of an inhibitor in the design of new medicines.^{10a} In the active site of CPA, the zinc ion coordinated tightly to the amino acid residues of His 69, Glu 72, and His 196 is essential for the enzyme reaction.^{10b} The guanidinium moiety of Arg 127 binds the oxyanion generated in the rate-limiting step of the formation of the tetrahedral transition state. Substrate specificity is brought about by a hydrophobic pocket and another guanidinium moiety of Arg 145.

In this paper, in continuation of work published in two short communications,⁹ the preparation of further artificial models for the natural enzyme carboxypeptidase A is described and the properties of this type of catalysts are discussed in detail. For this, new functional monomers, substrates, and imprinted polymers were prepared. The type and strength of interaction of functional monomers with the template in the presence or absence of Cu(II) are characterized more in detail. The catalytic activity of the imprinted polymers is discussed in relation to their chemical structure and the type of preparation. The optimized catalysts possess a remarkably high catalytic activity surpassing that of the corresponding catalytic antibodies by 2.5 orders of magnitude. These are also by far the highest catalytic activities found for catalysts based on molecularly imprinted polymers. The highest activity is obtained with a new type of dimeric binding site containing only one Cu²⁺ center.

This type of research provides more information for the understanding of the catalysis of natural enzymes, since these models show not only high catalytic activity but also other typical enzyme properties such as selectivity, Michaelis–Menten kinetics, high efficiency, high proficiency, competitive inhibition, and a bell-shaped pH rate profile.

2. Experimental Section

2.1. General Procedures. All reagents were reagent grade and were used without further purification, unless otherwise noted. Solvents were purified by standard methods. Column chromatography was carried out on silica gel 60 (70–230 mesh). NMR spectra were recorded using a Bruker AC250F operating at 500 MHz for ¹H NMR and 125 MHz for ¹³C NMR. IR spectra were recorded on a Bruker IFS-FT66V infrared spectrometer. Elemental analyses were determined on a Perkin-Elmer 240 DS elemental analyzer.

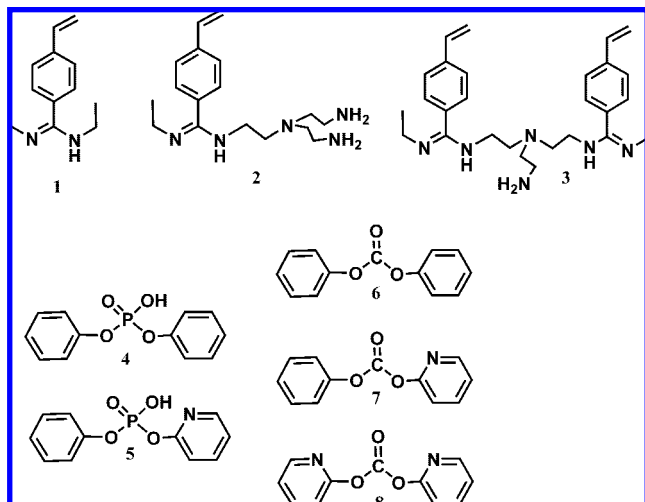
2.2. Syntheses of Templates and Substrates. The synthesis of the template **5** and the substrates phenyl-(2-pyridyl)-carbonate (**7**) and di-(2-pyridyl)-carbonate (**8**) (Chart 1) were described previously in our recent communication (see Supporting Information in ref 9a).

2.3. Syntheses of Monomers. The preparation of the new monomer *N,N*-[*N'*-(2-aminoethyl)-1,5-(3-azapentylen)]-bis[*N'*-ethyl-4-vinylbenzamidinium] (**3**) is performed in a similar manner as

- (6) (a) Wulff, G. *Angew. Chem.* **1995**, *107*, 1958–1979; *Angew. Chem., Int. Ed.* **1995**, *34*, 1812–1832. (b) Cormack, P. A. G.; Mosbach, K. *React. Funct. Polym.* **1999**, *41*, 115–124. (c) Shea, K. J. *Trends Polym. Sci.* **1994**, *5*, 166–173. (d) Sellergren, B., Ed. *Molecularly Imprinted Polymers. Man-made Mimics of Antibodies and Their Application in Analytical Chemistry*; Elsevier: Amsterdam, 2000. (e) Haupt, K.; Mosbach, K. *Chem. Rev.* **2000**, *100*, 2495–2504. (f) Wulff, G. In *Templated Organic Synthesis*; Diederich, F., Stang, P. J., Eds.; Wiley-VCH: Weinheim, 2000; pp 39–73.
- (7) (a) Robinson, D. K.; Mosbach, K. *J. Chem. Soc., Chem. Commun.* **1989**, 969–970. (b) Beach, J. V.; Shea, K. J. *J. Am. Chem. Soc.* **1994**, *116*, 379–380. (c) Ohkubo, K.; Urata, Y.; Honda, Y.; Nakashima, Y.; Yoshinaga, K. *Polymer* **1994**, *35*, 5372–5374. (d) Sellergren, B.; Karmalkar, R. N.; Shea, K. J. *J. Org. Chem.* **2000**, *65*, 4009–4027. (e) Svenson, J.; Zheng, N.; Nicholls, I. A. *J. Am. Chem. Soc.* **2004**, *126*, 8554–8560. (f) Maddock, S. C.; Pasetto, P.; Resmini, M. *Chem. Commun.* **2004**, 536–537.
- (8) (a) Wulff, G.; Gross, T.; Schönfeld, R. *Angew. Chem.* **1997**, *109*, 2049–2052; *Angew. Chem., Int. Ed. Engl.* **1997**, *36*, 1962–1964. (b) Strikowsky, A. G.; Kaspar, D.; Grün, M.; Green, B. S.; Hradil, J.; Wulff, G. *J. Am. Chem. Soc.* **2000**, *122*, 6295–6296. (c) Emgenbroich, M.; Wulff, G. *Chem. Eur. J.* **2003**, *9*, 4106–4117. (d) Wulff, G.; Chong, B.-O.; Kolb, U. *Angew. Chem.* **2006**, *118*, 3021–3024; *Angew. Chem., Int. Ed.* **2006**, *45*, 2955–2958.
- (9) (a) Liu, J.-Q.; Wulff, G. *J. Am. Chem. Soc.* **2004**, *126*, 7452–7453. (b) Liu, J.-Q.; Wulff, G. *Angew. Chem.* **2004**, *116*, 1307–1311; *Angew. Chem., Int. Ed.* **2004**, *43*, 1287–1290.

- (10) (a) Christianson, D. W.; Lipscomb, W. N. *Acc. Chem. Res.* **1989**, *22*, 6269–6300. (b) Philips, M. A.; Fletterick, R.; Rutter, W. J. *J. Biol. Chem.* **1990**, *265*, 20692–20698.

Chart 1. Structures of Designed Functional Monomers (1–3), Templates (4 and 5), and Substrates (6–8)



that of the monomer *N*-{2-[bis(2-aminoethyl)amino]ethyl-}*N*'-ethyl-(4-vinylbenzamide) (**2**) (for synthesis of **2**, see Supporting Information in ref 9a).

Thus dry tri-(2-aminoethyl)ammonium chloride (4.30 g, 0.021 mol) was added to a solution of *N*-ethyl-4-vinylbenzocarbamide ethyl ester^{6f} (8 g, 0.044 mol) in dry EtOH (150 mL) under argon. After stirring for 5 h, 4-*tert*-butylbenzocatechol (0.45 g) was added, the stirring was continued for 5 days at room temperature, and the solvent was removed in vacuo. The residue was treated with ice cooled 6 M NaOH (200 mL) and immediately extracted four times with ice cooled chloroform. The combined organic phases were dried with Na₂SO₄. The solvent was removed in vacuo, and the residue was purified by silica gel column chromatography using a 1:1 CH₂Cl₂/MeOH (MeOH saturated with NH₃) solution as the eluent to give a yellow liquid of **3** (2.01 g, 21% yield). FT-IR (KBr, cm⁻¹): $\nu = 3336$ (NH₃), 3269 (NH), 2944 (CH₃), 2886, 2848 (CH₂), 1623 (C=N amidine), 1605 (arom), 1507 (C=N amidine), 1460, 1444, 1305, 1135, 985, 916. ¹H NMR (CDCl₃, 25 °C): δ (ppm) = 7.51 (d, *J* = 7.8 Hz, 4H), 7.35 (d, *J* = 7.8 Hz, 4H), 6.68 (dd, *J* = 10.8 Hz, 2H), 5.82 (d, *J* = 17.6 Hz, 2H), 5.38 (d, *J* = 11.0 Hz, 2H), 2.52–3.84 (m, CH₂'s, 16H), 1.21 (t, *J* = 7.2 Hz, 6H). MS (FAB + NBA): *m/z*: 461 [M + H]⁺. Elemental analysis calculated (%) for C₂₈H₄₀N₆·2HCl (460.7 + 72.9): C, 63.04; H, 7.88; N, 15.76. Found: C, 62.80; H, 8.50; N, 16.01.

2.4. Synthesis and Properties of Imprinted Polymers.

2.4.1. Polymerization in the Presence of Copper(II) Ions. As a typical example the preparation of the imprinted polymer with monomer **3** and template **5** is described. Sodium phenyl-2-pyridylphosphate was transferred into the potassium salt with a cation ion-exchanger column (Amberlite IR-120). Potassium phenyl-2-pyridylphosphate (380 mg, 1.32 mmol) and monomer **3** (303 mg, 0.66 mmol) were dissolved in methanol (20 mL). The potassium salt was used since NaCl is known to have a relatively high solubility in methanol. After filtering off the KCl, an equivalent of CuCl₂ (88 mg) was dissolved in this solution under stirring for 10 min and the solvent was removed in vacuo to yield the Cu(II) complex of functional monomer **3** and template **5**. The complex obtained was dissolved in a mixture of MeCN (5.0 mL), DMSO (5.0 mL), EDMA (4 g), MMA (0.5 g), and AIBN (50 mg). For solubility reasons we selected a mixture of solvents MeCN/DMSO (1:1, v/v) as porogen. The reaction mixture was transferred to a 25 mL thick-walled ampule and was degassed by three freeze–thaw cycles under vacuum and then sealed. The polymerization was performed at 60 °C for 3 days. After crushing, the polymer was washed with methanol and dried under vacuum. The crushed polymers were ground using a mill and sieved to obtain 45–250 μ m particles. The template was removed by exhaustive washing with a mixture

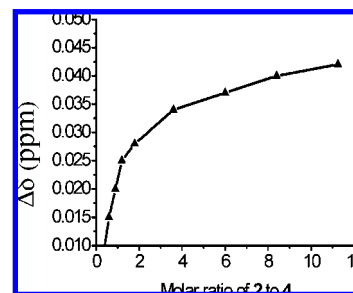


Figure 1. Saturation plot of the complexation of the functional monomer **2** and the template **4** (DPP). Data were obtained by ¹H NMR titration; the changes in chemical shift of the phenyl ring protons at δ 7.23 were used as a reference.

of 0.2 M NaOH and acetonitrile (1:1, v/v) to give ~75% free cavities. The free cavities in the imprinted polymers were determined by measuring the complexation of diphenylphosphate (**4**) to the polymer at 25 °C (see determination of amidines with diphenylphosphate).

As a comparison, a control polymer with formic acid instead of the template was prepared in an analogous manner. For comparison purposes the imprinted polymers were also prepared with DMSO and with DMF as the porogen.

2.4.2. Substitution of Zn²⁺ by Cu²⁺ in a Zn²⁺-Imprinted Polymer. The preparation of imprinted polymers containing Zn²⁺ was performed as described previously (see Supporting Information in ref 9b). A suspension of freshly prepared Zn²⁺-imprinted polymer **PZn2,5** (100 mg) in a mixture of water and *N,N*-dimethylformamide (DMF) (1:1, v/v) (50 mL) was treated with EDTA·2Na⁺ (100 mg) to remove the Zn²⁺. The mixture was stirred at 100 rpm and room temperature for 1 day. The polymers were collected by filtration and washed with DMF, 0.2 M NaOH, and water. This procedure was repeated three times. The polymer was resuspended in DMF (20 mL) containing CuCl₂ (20 mg), and the mixture was stirred at 100 rpm at room temperature for 1 day. The polymers exhibiting a blue color were collected by filtration and washed with DMF and water and then dried in vacuo (**PZn2,5Cu**). A control polymer prepared with formic acid instead of the template was treated identically.

2.4.3. Potentiometric pH Titrations. Potentiometric pH titrations were performed using a standard electrode system (Orion Research Ross Combination pH Electrode 8100BN). The test solutions were prepared with freshly distilled water and were degassed under ultrasonic agitation. All of the test solutions (50 mL) were kept under an argon atmosphere. The potentiometric pH titrations of the monomer **2** (1.0 mm) in the absence and the presence of 1 equivalent of Cu(II), respectively, were carried out at 25 °C with *I* = 0.1 (NaNO₃), and at least two independent titrations were made for each system. The value of $K_w = [\text{H}^+][\text{OH}^-]$ at 25 °C and *I* = 0.1 (NaNO₃) was determined to be 10^{-13.79}. As a comparison, tris(2-aminoethyl)amine was used as a control (see Figure 3 in Results and Discussion).

2.4.4. ¹H NMR Titration. Mixtures of different molar ratios (0.2–15) of the phosphate (DPP) **4** to the functional monomer **2** in CDCl₃ or MeCN-*d*₃ were prepared in 10 NMR tubes and analyzed. After equilibration for 20 min, the relative changes in the chemical shifts of **4** were plotted as a function of the molar ratio of **2** to **4**. The titration experiments yielded a saturation isotherm (Figure 1). Nonlinear regression analysis led to apparent complex constants (K_s). The stoichiometry of the complex formation between **4** and the functional monomer **2** was determined with a Job plot (Figure 2).

2.4.5. Determination of the Amidinium Groups and Their Complexing Ability in MIPs. The content of the amidinium groups in the polymers was determined by the complex formation of diphenylphosphate (**4**) with the amidinium groups in MeCN solution

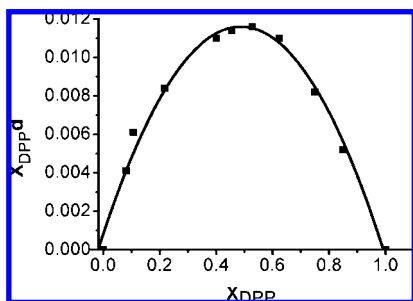


Figure 2. Job plot of the complexation of **2** and **4** by ^1H NMR titration as in Figure 1. X_{DPP} = mole fraction of diphenylcarbonate **4** (DPP), $X_{\text{DPP}}\Delta$ = mole fraction X multiplied by Δ .

(see ref 11). Polymer samples (10 mg each) were suspended in MeCN solution (1 mL) in screw-cap vials, after addition of different amounts of **4** (resulting in 0.28, 0.7, 1.4, 2.8, 4.2, and 8.4 mM solutions), the vials were stirred at room temperature for 24 h, then the polymer was removed by filtration, and the remaining **4** in the solution was determined by UV spectroscopy at 260 nm ($\epsilon = 5.79 \times 10^2 \text{ M}^{-1} \text{ cm}^{-1}$). The amidinium group content and the complexation constants of the diphenylphosphate (**4**) with the amidinium binding site can be analyzed with nonlinear regression of the plot of the concentration of occupied binding sites against the concentration of guest **4**. The amidinium group content can also be determined by N -elemental analysis.

2.4.6. Determination of Cu^{2+} Content in the MIPs. The content of copper ions in the imprinted polymers was determined by elemental analysis for copper. The copper content can also be calculated from the triamine content. In this case, the triamine moiety in the polymer was determined by N -elemental analysis, and the copper content was calculated to be equimolar to the triamine content assuming that the triamine moiety and Cu^{2+} forms a 1:1 complex in MIPs. Both methods gave equivalent values.

2.4.7. Hydrolyses of Substrates. The hydrolyses of the carbonates **6**, **7**, and **8** were carried out in a 1:1 solution of 50 mM HEPES buffer (pH 7.3) and MeCN at 20 °C. The formation of phenol or pyridone was followed by HPLC (Waters 410 pump, Waters 486 UV-detector, integration software CSW from Apex Data) analysis on a reversed-phase column (RP-18, Merck). The inherent reactivities of the three carbonate substrates against water at pH 7.3 are quite different. Thus the k_{uncat} of **6**, **7**, and **8** were found to be 7.20×10^{-7} , 2.60×10^{-5} , and $2.55 \times 10^{-4} \text{ min}^{-1}$, respectively. In a typical experiment for the hydrolysis of di-(2-pyridyl)carbonate (**8**), 0.1–1 mg of dry polymer was added to 1 mL of a buffer–MeCN solution in a screw-cap vial, and the mixture was stirred at 20 °C for several hours. After equilibration, the reaction was initiated by injecting 20 μL of 0.5 mM **8** in dry acetonitrile (the final concentration of **8** was 0.01 mM), and 50 μL of the reaction mixture were taken at regular intervals and quickly filtered to remove the polymer and analyzed by HPLC. Considering the effect of the pH on the products, MeCN/potassium phosphate buffer 0.01 M (70:30 v/v) at pH 7.4 was used as the mobile phase. The flow rate was 1.5 mL/min. The UV detection was performed at 218 nm. Pseudo-first-order rate constants k for the hydrolysis were determined from the slopes of semilogarithmic plots of the reaction progress against the time.

2.4.8. Kinetics. For the determination of the Michaelis–Menten kinetics, plots of initial velocities of the catalyzed hydrolysis versus substrate concentration were measured. In these investigations the initial reaction rates were monitored while maintaining a constant concentration of active sites and increasing substrate concentrations. The procedure to measure the velocity was analogous to pseudo-first-order kinetics as described. The saturation plots of the

hydrolysis of **8** by the imprinted polymer **PCu3,5** and by the control polymer is shown in Figure 5 (Results and Discussion). From that, Michaelis–Menten kinetics were calculated from the double-reciprocal (Lineweaver–Burke) plots for the hydrolysis of **8** catalyzed by **PCu3,5** or by fitting the Michaelis–Menten kinetics to a hyperbola using the program Origin 7.0. The competitive inhibition of the hydrolysis by the template **5** was carried out by adding different amounts of inhibitor **5**. The molar ratios of the active sites of the MIP **PCu2,5** to **5** were 1:0, 2:1, and 1:10 (Figure 6).

3. Results and Discussion

3.1. Rational Design and Synthesis. Enzymes are essentially flexible molecules evolved over a very long time; they are precisely complementary to the reactants in their activated transition state geometry.¹² Although this notion stated by Pauling 60 years ago has gradually come to be accepted, debates still continue about the precise nature of enzyme catalysis.¹³ To elucidate the important role of transition state stabilization in enzyme catalysis, two major strategies have been developed and they actually represent important progress in the present understanding of enzyme mechanisms. In this regard the groups of Lerner and Schultz independently showed the first successful examples by generating antibodies against a stable transition state analogue (TSA). These antibodies show considerable catalytic activity.³ The other remarkable development is the preparation of polymers imprinted by TSAs which display a significant catalytic capacity.^{5–9} Enzyme-like activity by transition state stabilization was thus clearly demonstrated in two different systems.^{3,5}

In our previous work⁸ in designing polymer catalysts by molecular imprinting, the functional amidinium group N,N' -diethyl-4-vinylphenylamidinium (**1**) was rationally positioned by using phosphonate or phosphates as templates. In the hydrolysis of esters, carbonates, and carbamates, rate enhancements of 100–3000-fold were obtained using TSA imprinted polymers. The amidinium group acted as a transition state binding site similar to the catalytic action of Arg 127 in carboxypeptidase A (CPA) catalysis.

On the basis of these positive results for TS stabilization, we made further efforts to adjust the active site of our molecularly imprinted polymers (MIPs) to that of carboxypeptidase A (CPA). For these experiments, carbonate hydrolysis was selected as the model reaction (Scheme 1). Stable analogues of the structurally well-characterized tetrahedral transition states for this reaction have been widely used in the preparation of the corresponding catalytic antibodies.^{3a,b} In our case the functional monomer **2** was chosen since it is expected to form a stable complex with the phosphate group of template **5**. An additional triamine group was introduced with a defined proximity to the amidinium group. This group gives rise to a strong 3-fold coordination of Zn^{2+} or Cu^{2+} ion leaving the fourth or fifth coordination site free for other ligands.⁹ The monomer **2** was synthesized as shown in Scheme 2 (see Supporting Information^{9b}). Thus, the main catalytic factors of CPA, an amidinium (instead of a guanidinium) group and a Zn^{2+} center, were introduced in a TSA imprinted polymer cavity. The imprinted polymers exhibited strong rate enhancements $k_{\text{catt}}/k_{\text{soln}}$ for carbonate hydrolysis by

(11) Jang, B.-B.; Lee, K.-P.; Min, D.-H.; Suh, J. *J. Am. Chem. Soc.* **1998**, *120*, 12008–12016.

(12) (a) Pauling, L. *Chem. Eng. News* **1946**, *24*, 1375–1377. (b) Pauling, L. *Nature* **1948**, *161*, 707–709. (c) Jencks, W. *Catalysis in Chemistry and Enzymology*; McGraw-Hill: New York, 1969.

(13) (a) Warshel, A. *J. Biol. Chem.* **1998**, *273*, 27035–27038. (b) García-Viloca, M.; Gao, J.; Karplus, M.; Truhlar, D. G. *Science* **2004**, *303*, 186–195. (c) Gao, J. *Curr. Opin. Struct. Biol.* **2003**, *13*, 184–192.

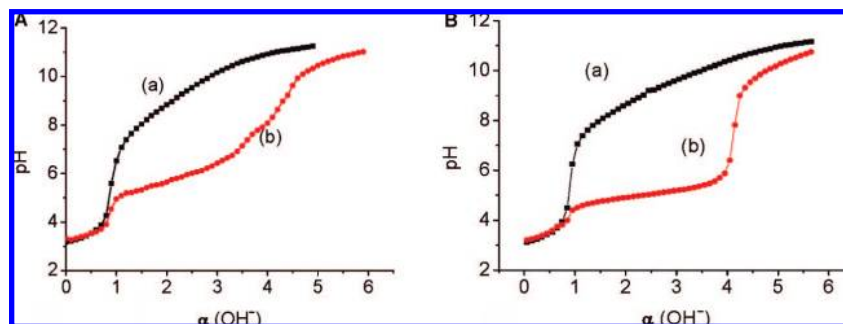


Figure 3. Potentiometric pH titration curves. (A) (a) 1 mM $2\cdot 4H^+$ at $I = 0.10$ ($NaNO_3$), and (b) 1 mM $2\cdot 4H^+$ + 1.00 mM $CuCl_2$ at $I = 0.10$ ($NaNO_3$). (B) For comparison the potentiometric pH titration curves are given for (a) 1 mM tris(2-aminoethyl)amine· $4H^+$ at $I = 0.10$ ($NaNO_3$), and (b) 1 mM tris(2-aminoethyl)amine· $4H^+$ + 1.00 mM $CuCl_2$ at $I = 0.10$ ($NaNO_3$). $\alpha(OH^-)$ represents the number of moles of base (0.1 mM NaOH) per mole of ligand.

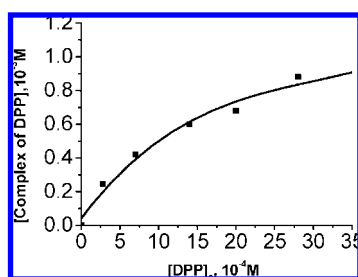


Figure 4. Plot of the concentration of the occupied binding sites versus that of the guests. Measured is the complexation of **4** (DPP) to the template-free imprinted polymer **PCu2,5** at 25 °C. The concentration of the complexes was calculated by spectrophotometrically detecting the uncomplexed **4** (DPP) in MeCN ($\lambda = 260$ nm, $\epsilon = 5.79 \times 10^2$ M $^{-1}$).

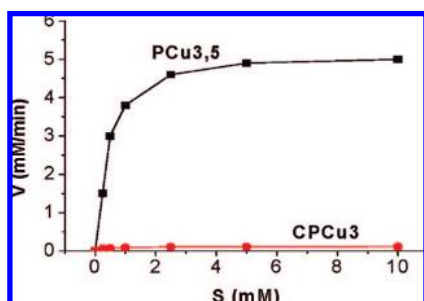


Figure 5. Michaelis–Menten plot of the hydrolysis of **8** by the imprinted polymer **PCu3,5** measured with **PCu3,5** (0.051 mM of available cavities) in buffer solution (HEPES/MeCN 1:1) (■) and by the nonimprinted polymer **CPCu3** (0.098 mM of available Cu^{2+} in the polymer) (●), pH = 7.3 at 20 °C.

a factor of 6900. By the replacement of Zn^{2+} by Cu^{2+} in the imprinting procedure, a further dramatic catalytic rate enhancement of 110 000-fold was observed.^{9a}

For further improvement of the catalysis, the new monomer **3** was designed to introduce one Cu^{2+} center and two amidine groups in one imprinted cavity (Scheme 2). This design changed the binding of the substrates and, more importantly, the type of coordination of the copper in the active site as well as the reactivity of the copper bound HO^- and H_2O . This should increase the binding and catalysis in the imprinted cavities. The novel design led to further enhancement of the catalytic activity.

The functional monomer **3** was synthesized in a similar way as **2** (Scheme 2). *N*-Ethyl-4-vinylphenylamide is treated with triethyloxoniumtetrafluoroborate to yield *N*-ethyl-4-vinylbenzocarbonyl ester. Reaction of this compound with an equimolar amount of tris(2-aminoethyl)amine yielded the

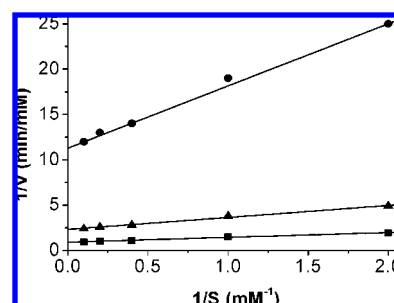


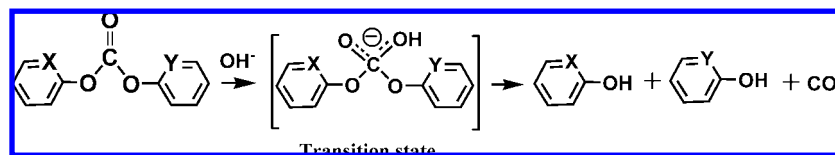
Figure 6. Double-reciprocal plots (Lineweaver–Burke) for the catalyzed hydrolysis of **8** and the inhibition by the template. Inhibition studies of the hydrolysis of **8** in presence of **PCu2,5** using the original template **5** as an inhibitor in a 1:1 solution of HEPES buffer (pH 7.3) and MeCN at 20 °C. The molar ratio of the active sites to the inhibitor was (■) 1:0; (▲) 2:1; (●) 1:10. The inhibition constant was calculated to be $K_i = 25$ μM .

monomer **2**; the monomer **3** could be obtained by reaction of 1 equiv of tris(2-aminoethyl)amine with 2 equiv of *N*-ethyl-4-vinylbenzocarbonyl ester.

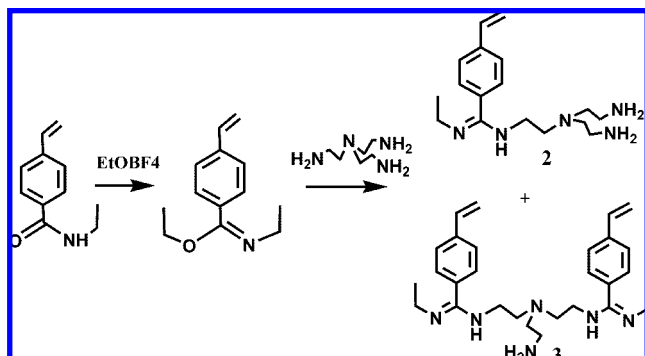
Initially, diphenylphosphate (**4**) was used as template for catalysts for the carbonate hydrolysis.^{8b} The new template **5** proved to be much more efficient.⁹ One phenyl ring in **4** was replaced by a 2-pyridyl ring in **5**. This change gives the possibility of incorporating the pyridine nitrogen atom as the fourth ligand in the Cu^{2+} coordination sphere (see Scheme 4). The additional coordination permits the formation of more stable complexes between the functional monomer and the template during polymerization. Furthermore, the amidinium group and the Cu^{2+} ion are brought into defined proximity to each other and to the template molecule in the cross-linking polymerization during the imprinting process. The template **5** was synthesized as shown in Scheme 3. The attempt to prepare the new template di-2-pyridyl phosphate failed owing to its instability.

The reactivity of the substrates varied clearly with the template structure used during imprinting. In our earlier study,^{9b} the template **5** and the substrate **6** were first used in the catalysis with the imprinted polymers. In order to design a substrate that is more similar to the template, the substrate phenyl-(2-pyridyl)carbonate (**7**) and di-(2-pyridyl)carbonate (**8**) were synthesized.^{9a} This led to a better binding of the substrate in the imprinted cavity compared to **6**, since the nitrogen of the pyridyl ring can interact with the Cu^{2+} center similarly to the template **5** described above. The synthesis of **8** is readily achieved by the reaction of triphosgene with 2-hydroxypyridine. Substrate **8** is inherently more reactive toward water than **7**; substrate **6** shows the lowest reactivity.

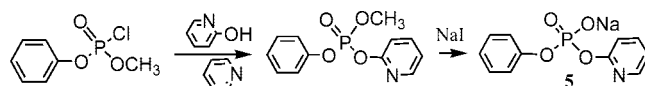
Scheme 1. Hydrolysis of Carbonate



Scheme 2. Synthesis of Functional Monomers



Scheme 3. Synthesis of the Template 5



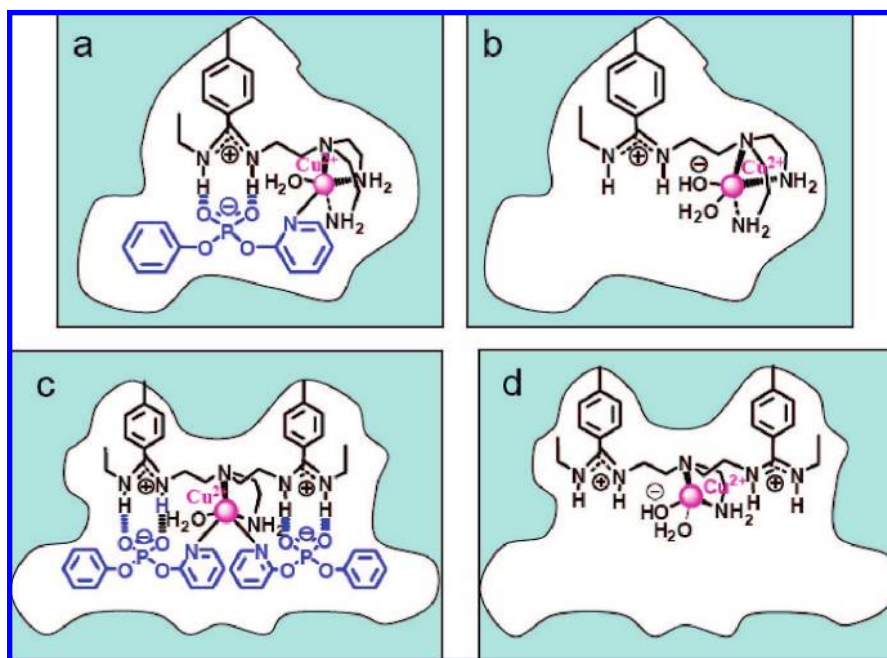
3.2. Characterization of the Complexation of the Functional Monomers with the Template. Stoichiometric noncovalent interaction combines the advantages of covalent and noncovalent interaction during the molecular imprinting procedure and generates high association constants between TSA and the functional monomer.^{5a} As shown in previous studies,^{5a,14} the amidinium group can bind strongly to carboxylic acids, phosphonic acids, and phosphates under imprinting conditions. This fact allows fixing a stable transition state analogue template through multiple hydrogen bonds and electrostatic interactions and to position the amidine groups in a correct orientation for catalysis. For the characterization of this type of complexation, ¹H NMR spectroscopy has proven to be an excellent tool.¹⁴ The formation of the complex of the functional monomer and the template (for example, between **2** and **4**) was studied by ¹H NMR titration experiments yielding a saturation isotherm (Figure 1). Changes in the chemical shift of the benzene ring protons (δ 7.23) of the template were used as a reference for electrostatic and hydrogen interaction between the functional monomer and the template. Job plot analysis^{14,15} of the complexation demonstrated a 1:1 complexation between the functional monomer and the template (Figure 2). The apparent association constant of **2** and **4** was determined to be $5.3 \times 10^3 \text{ M}^{-1}$ in acetonitrile-*d*₃ (MeCN) by ¹H NMR spectroscopic titration; a similar result was also observed in CDCl₃ ($5.6 \times 10^3 \text{ M}^{-1}$). In the case of the complexation of **1** and **4** the association constant was determined to be $4.6 \times 10^3 \text{ M}^{-1}$ in MeCN at 25 °C.¹⁴ The complexation of **2** and **5** showed an association constant of $1.1 \times 10^4 \text{ M}^{-1}$ in acetonitrile; it is somewhat higher than that between **2** and **4**. The binding of the functional monomer **2** and **5** in the presence of Cu²⁺ can also be observed in acetonitrile by ¹H NMR at a relatively low concentration of the copper

complexes. The observed large change in the chemical shift on complexation implied a strong binding in the presence of Cu²⁺, but at higher concentrations, the complexes partially precipitated from the solution. Therefore, it was not possible to determine with some accuracy the association constant of **2** and **5** in the presence of Cu²⁺ by ¹H NMR titration. However, it is to be expected that the complexation of **2** with **5** in the presence of Cu²⁺ is much stronger than that of **2** and **5** alone owing to the strong binding of the Cu²⁺ ion with the pyridine ring of template **5**.

The complexation of Cu²⁺ ions with the triamine part of monomer **2** was characterized by potentiometric titration in aqueous solution (Figure 3A). From the potentiometric titration a high stability constant of 10^{15} M^{-1} was found, a value that is in accordance with other observations in similar systems.¹⁶ In the case of the reference substance, tris(2-aminoethyl)amine, a smooth and clear titration curve in the presence of Cu²⁺ showed that four protons were neutralized at $\alpha(\text{OH}^-) = 4$, implying a tetra coordination of the tetraamine for Cu²⁺ (Figure 3B). However, the curve for the complexation of monomer **2** is quite different (Figure 3A,b). The complexation below $\alpha(\text{OH}^-) = 3$ is similar to the foregoing example, but above $\alpha(\text{OH}^-) = 3$, the curve is different and indicates partial neutralization of other kinds of protons. This result reflects a strong tricoordination of the Cu²⁺ with the triamine part of monomer **2**. In comparison with similar known copper complexes^{2e,f} a pentacoordinated copper with two additional oxygen ligands (OH⁻, H₂O) can be assumed. The exact stereochemistry with regard to the position of the ligands in the complex is not known. An X-ray crystallographic investigation should bring more information in this respect. Other types of coordination of Cu²⁺ are much weaker. It is known that only a weak coordination of Zn²⁺ to amidinium groups of similar systems is occurring.¹⁷ A weak binding of the copper to the amidinium ion would facilitate the complexation of the amidinium ion to the phosphate template. On the basis of these binding studies and considering the solubility, the copper ion complexes for molecular imprinting were prepared in MeCN/DMSO (1:1, v/v), although in this mixed solvent lower association of phosphate with amidinium was observed compared to pure MeCN.

3.3. Synthesis and Characterization of Imprinted Polymers. Highly cross-linked molecularly imprinted polymers were prepared in bulk by standard procedures using the TSA **5** as a template, **2** or **3** as functional monomers, and ethylene dimethacrylate (EDMA) as a cross-linker in the presence of Cu²⁺ (Scheme 4a and c). Some methyl methacrylate is added in order to improve the flexibility of the resulting polymer. The copper monomer–template complex is prepared by dissolving the potassium salt of the template **5**, the monomer **2** or **3**, and an equimolar amount of CuCl₂ in methanol. Potassium(I) in **5** is replaced by copper(II), and KCl precipitates. For solubility reasons the porogen has to contain a certain amount of a polar

(14) Wulff, G.; Knorr, K. *Bioseparation* **2002**, *10*, 257–276.(15) (a) Takeuchi, T.; Dobashi, A.; Kimura, K. *Anal. Chem.* **2000**, *72*, 2418–2422. (b) Striegler, S. *Bioseparation* **2001**, *10*, 307–314.(16) Zompa, L. J. *Inorg. Chem.* **1978**, *17*, 2531–2536.(17) Kimura, E.; Shiota, T.; Koike, T.; Shiro, M.; Kodama, M. *J. Am. Chem. Soc.* **1990**, *112*, 5805–5811.

Scheme 4. Schematic Representation of the Preparation and the Catalytic Centers of Imprinted Polymer Catalysts^a

^a (a) Molecular imprinting with functional monomer **2** and the template **5** in presence of Cu^{2+} for the preparation of the imprinted polymer catalyst **PCu2,5**. (b) The enzyme-like active site of **PCu2,5** prepared after removal of the template **5**. (c) Molecular imprinting with functional monomer **3** and two molecules of the template **5** in presence of Cu^{2+} for the preparation of the imprinted polymer catalyst **PCu3,5**. (d) The enzyme-like active site of **PCu3,5** after removal of the template **5**.

solvent such as DMSO or DMF. Therefore, the solvent acting as a porogen consisted of a mixture of acetonitrile and DMSO (1:1, v/v); in other experiments either pure DMSO or DMF was used. It is interesting that the copper content in the polymerization mixture does not significantly inhibit the radical polymerization. After polymerization and grinding, the templates were removed from the polymer particles (45–125 μm) to give ~75% free cavities (Scheme 4b). The control polymers with identical composition to that of the imprinted polymer but with formic acid instead of the template were synthesized in an analogous manner. The method mentioned above was demonstrated to be an efficient one for constructing Cu(II)-containing active cavities (Scheme 4).

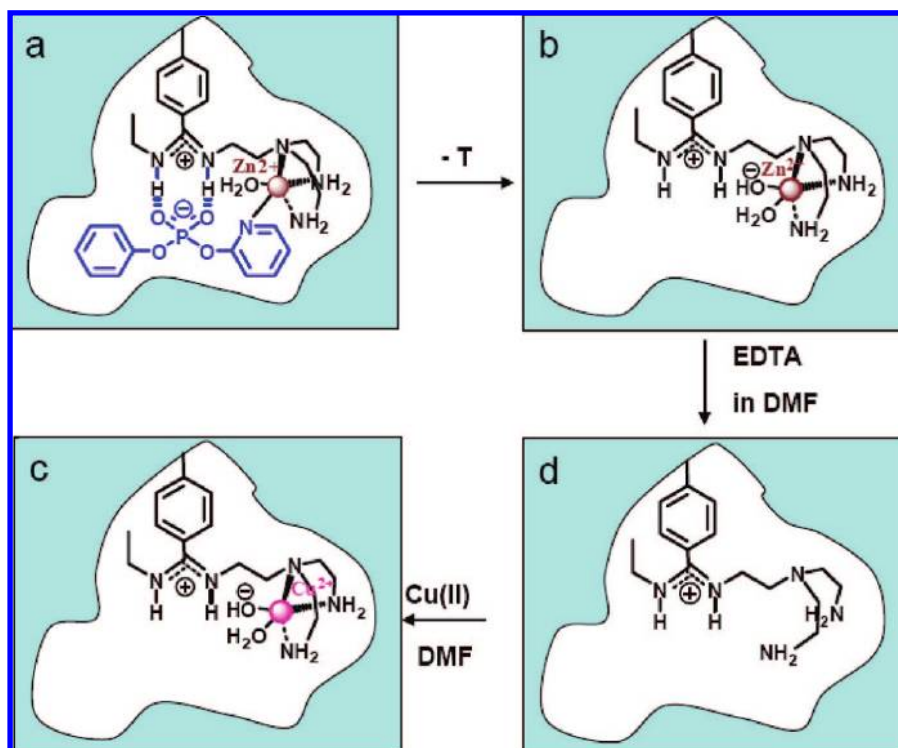
In order to compare the catalytic activity of different metal ions such as Cu(II) and Zn(II), imprinted catalysts were prepared from both metals. The catalytic activity proved to be very different, and the question arose whether this is due to special imprinting effects of the metal ions or if this is mainly dependent on the inherent catalytic property of the metal ions themselves. To investigate this question an alternative strategy for the preparation of Cu(II)-containing imprinted polymers was developed by substitution of Zn(II) by Cu(II) in Zn(II)-imprinted polymers (Scheme 5). The Zn(II)-containing imprinted polymer **PZn2,5** was synthesized as described previously.^{9b} The Zn(II) was removed by a 10-fold excess of $\text{EDTA} \cdot 2\text{Na}^+$ and reloaded by Cu(II). The Cu(II)-containing, blue colored polymer **P(Zn)2,5Cu** was obtained. Another model system containing two amidinium groups (corresponding to two guanidinium groups in carboxypeptidase A) was obtained using a complex of the functional monomer **3** with 2 equiv of template **5** in the presence of Cu(II) (Scheme 4c, d). The imprinted polymer **PCu3,5** was prepared analogously as described for **PCu2,5**. The active site in the imprinted polymer is shown in Scheme 4d.

The surface areas of the prepared polymers were determined by BET analysis (N_2 , one point measurement), and high inner

surface areas typical for macroporous polymers were obtained. Comparable inner surface areas for the imprinted and the nonimprinted control polymers were observed, for example, 310 m^2/g for **PCu2,5** and 290 m^2/g for **CPCu2,5**; 390 m^2/g for **PCu3,5** and 320 m^2/g for **CPCu3,5**. This shows that the polymer structure of imprinted and control polymers are quite similar, and a comparison of the catalytic properties should mainly rely on the imprinting effect of the active site. From comparison of polymers prepared from monomer **2** and monomer **3**, the polymers from the latter show a somewhat higher inner surface area for both imprinted and control polymers. The reason may be that **3** is also a cross-linker and may influence the polymer structure to some extent. A higher surface area results in a better accessibility and may also influence the catalytic activity. This assumption can be made since from earlier investigations it is known that the porosity of the polymers prepared under these conditions allows a free diffusion within the pores.^{6a}

The content of copper(II) in the imprinted polymers was estimated by elemental analysis. No loss of Cu(II) ions was found during splitting off the template from the imprinted polymers; similar results had already been observed in the case of Zn(II)-imprinted polymers.^{9b} This observation was further supported by the fact that the content of triamine groups (calculated from elemental analysis) is nearly identical with that of Cu(II) in the imprinted polymer (e.g., 0.126 mmol/g triamine for **PCu2,5** and 0.131 mmol/g Cu(II) for **PCu2,5**).

The content of amidinium ions in the polymers was determined by measuring the extent of complexation of the amidinium ions with diphenylphosphate (DPP, **4**) in MeCN solution. This method was previously used in similar nonimprinted systems by Suh et al.¹¹ The plot of the complexation of **4** to the imprinted polymer **PCu2,5** is shown in Figure 4. From the analysis of the data with a nonlinear regression, the content of amidinium ions can be calculated. For example, 0.11 mmol/g

Scheme 5. Preparation of Imprinted Polymers by Substitution of Zn(II) by Cu(II) in Zn(II)-Imprinted Polymers^a

^a (a) Molecular imprinting with functional monomer **2** and the template **5** in presence of Zn(II) for the preparation of Zn(II)-imprinted polymer catalyst **PZn2,5**. (b) The imprinted cavity of **PZn2,5** after removal of the template; (d) Removal of Zn(II) from **PZn2,5** by EDTA in a mixture of DMF and water (1:1, v/v). (c) Reconstructed metal center with a Cu(II) in an originally Zn(II)-imprinted polymer (**PZn2,5Cu**).

amidinium groups in polymer **PCu2,5** and 0.12 mmol/g amidinium groups in **PCu3,5** were obtained. These values represent the available amidinium ions in the polymer. The total content of amidinium groups can also be calculated from the elemental analysis; for **PCu2,5** the content of amidinium groups is 0.136 mmol/g. Considering ~75% free cavities in the imprinted polymer, this analysis is in good agreement with the results of the complexation of amidine with diphenylphosphate **4**. The association constant (K_a) for the complex formed between **4** and the active site of the imprinted polymer **PCu2,5** was also estimated from the above experiments ($K_a = (1.65 \pm 0.5) \times 10^4 \text{ M}^{-1}$). This association is considerably higher compared to that for the complexation of the monomer **2** with **4** in MeCN ($K_a = (5.3 \pm 0.6) \times 10^3 \text{ M}^{-1}$). The result is not surprising considering both binding of the amidinium ion and a selective recognition derived from the imprinting effect (although **4** is similar to but not identical to the template).

3.4. Catalytic Activity of the Imprinted Polymers. The catalytic activity of the imprinted polymers was determined by investigating the rate of hydrolysis in the presence of these polymers for different carbonates in a 1:1 solution of HEPES buffer (pH 7.3) and MeCN. In order to follow the reaction kinetics, aliquots were taken at regular intervals and were analyzed by HPLC on a C₁₈-reversed-phase column. Phenol and 2-hydroxypyridine, as the reaction products, were determined quantitatively. The pseudo-first-order rate constants were measured at low conversion from the slopes of a semilogarithmic plot of reaction progress against time.⁹ k_{impr} is the pseudo-first-order rate constant in the presence of the imprinted catalyst, k_{contr} , in the presence of the control polymer, and k_{soln} , without catalyst just in solution of HEPES buffer (pH 7.3)/MeCN 1:1. As in previous studies⁹ the activity of the catalyst was expressed by the ratio of reaction in the presence of polymer catalyst to

that in neat buffer solution ($k_{\text{impr}}/k_{\text{soln}}$). Effects that are only connected to the imprinting in the polymer can be elucidated from the ratio $k_{\text{impr}}/k_{\text{contr}}$; this is designated as the imprinting factor.

It had been shown⁹ that the introduction of metal ions into the TSA-imprinted active site resulted in a strong increase in catalytic activity. Thus the value of 455 for $k_{\text{impr}}/k_{\text{soln}}$ for the hydrolysis of diphenylcarbonate (**6**) in the presence of **P1,4**^{8b} increased on introduction of Zn²⁺ (**PZn2,5**) by a factor of 7 and $k_{\text{impr}}/k_{\text{contr}}$ by a factor of 6.^{9b} The increase was even stronger in the case of introduction of Cu²⁺ (**PCu2,5**). $k_{\text{impr}}/k_{\text{soln}}$ increased by a factor of 18. It is interesting that additional “free” Cu²⁺ or Zn²⁺ ions do not have a significant influence on the rate. This is also true if these metal ions are added to the neat buffer solution.

Now the catalytic activity of imprinted polymers prepared with two different methods has been compared for the hydrolysis of phenyl-2-pyridyl-carbonate (**7**). This substrate is more similar to the template used during imprinting, and therefore the catalytic activities of the imprinted catalysts toward **7** are considerably higher. In Table 1 the catalytic activity of Cu(II) and Zn(II) imprinted catalysts are compared. The Zn(II) imprinted catalyst showed a $k_{\text{impr}}/k_{\text{soln}}$ of 4040, and the Cu(II) imprinted catalyst, that of 15700. Also the imprinting factors are quite high with 63.2 and 76.9, respectively. If the polymer is imprinted with Zn(II), and then the Zn(II) is substituted by Cu(II), the catalytic activity was lower as in the case of direct imprinting with Cu(II) (Table 1). This result is consistent with the complexing ability of the two systems during imprinting. The Cu(II) complex of the triamine part of monomer **2** showed a very high association constant of $10^{15.8} \text{ M}^{-1}$, compared to $10^{9.3} \text{ M}^{-1}$ between triamine of **2** and Zn(II).^{9a} Furthermore, Cu(II) also displays a stronger capacity to complex the pyridine

Table 1. Pseudo-First-Order Kinetics of the Hydrolyses of Carbonates **7** and **8** in Presence of Different Catalytically Active Imprinted Polymers Containing Zn(II) and Cu(II)

imprinted polymer ^a	substrate	k_{impr} (min ⁻¹) ^b	$k_{\text{impr}}/k_{\text{soln}}$	$k_{\text{impr}}/k_{\text{contr}}$
PZn2,5	7	0.105	4040	63.2
PZn2,5Cu	7	0.241	9250	57.8
PCu2,5^c	7	0.41	15 700	76.9
PCu2,5^c	8	13.0	51 000	80.1
PCu3,5	7	2.56	98 200	50.2
PCu3,5	8	55.3	217 000	53.8

^a The imprinted polymer **PZn2,5** was prepared using monomer **2** and template **5** in the presence of Zn(II); **PZn2,5Cu** was obtained from **PZn2,5** by substitution of Zn(II) by Cu(II); **PCu2,5** or **PCu3,5** was prepared using monomer **2** or **3** and template **5** in the presence of Cu(II). ^b Hydrolyses of carbonates **7** or **8** in a solution of 50 mM HEPES buffer (pH 7.3)/MeCN 1:1 at 20 °C (HEPES = 2-[4-(2-hydroxyethyl)-1-piperazine]ethanesulfonic acid). There are 2 mM of available active sites in relation to 1 mM substrate; all k values are the average of at least three measurements. ^c Data from ref 9a.

Table 2. Pseudo-First-Order Kinetics of the Hydrolyses of Carbonate **7** by Imprinted Polymers Prepared by Using Different Porogens

imprinted polymer	porogen	k_{impr} (min ⁻¹) ^a	$k_{\text{impr}}/k_{\text{soln}}$	$k_{\text{impr}}/k_{\text{contr}}$
PCu2,5^b	MeCN/DMSO(1:1)	0.41	15700	76.9
PCu2,5	MeCN/DMSO(1:2)	0.195	7451	34.5
PCu2,5	DMSO	0.085	3220	15.8
PCu2,5	MeCN/DMF (1:1)	0.095	3630	17.8
PCu2,5	DMF	0.020	781	3.96

^a Hydrolysis of carbonate **7** in a solution of 50 mM HEPES buffer (pH 7.3) /MeCN 1:1 at 20 °C. There are 2 mM of available active sites in relation to 1 mM substrate. k_{impr} is the pseudo first-order rate constant in presence of the polymeric catalyst, k_{contr} is the rate constant in presence of the control polymer and k_{soln} the rate constant in the HEPES buffer (pH 7.3)/MeCN 1:1 solution, all values are means of at least three times. ^b Data from ref 9a.

moiety of **5** than Zn(II). This result shows that the higher catalytic activity is dependent not only on the better catalytic properties of Cu(II) but also on the better imprinting properties of the copper ion. Thus, the stable complexation between monomer and template provided a better defined conformation of the complex and a better binding during the imprinting procedure. A strong binding of the TSA to the imprinted catalyst during the reaction would exhibit high catalytic efficiency for the reaction. This result is in good agreement with the notion regarding TS stabilization in enzymatic catalysis. Furthermore it shows that similarly, as with Zn²⁺, the copper ions do not appreciably interfere in the radical polymerization.

In order to obtain more information on the effect of the porogen used during the preparation of the imprinted polymers on the catalytic activity, different solvents were used as reaction medium as shown in Table 2. Different porogens led to a remarkable change of the catalytic activity of the imprinted polymers. Using polar solvents as the porogen, poorer catalytic activities and imprinting effects were observed. For example, in pure DMF an imprinting effect of 3.96 for **PCu2,5** and low catalytic activity were obtained. On addition of MeCN to the DMF using a mixture of solvents the properties improved somewhat. DMSO as a solvent seems to be better; a relatively high imprinting factor of 15.8 was obtained with pure DMSO as a porogen. This is considerably improved by using a mixture as a porogen with added MeCN. In the case of a 1:1 mixture of MeCN and DMSO as the porogen, a high imprinting factor of 76.9 was observed (Table 2). The attempt to use pure MeCN

Table 3. Comparison of Michaelis–Menten Kinetics and K_{ix}^{-1} (Catalytic Proficiency) of Hydrolyses of Carbonate **8** with Imprinted Polymers and Control Polymers

polymer ^a	k_{cat} (min ⁻¹)	K_{m} (mM)	$k_{\text{cat}}/k_{\text{unecat}}$	$k_{\text{cat}}/K_{\text{m}}$ (min ⁻¹ M ⁻¹)	K_{ix}^{-1} (M ⁻¹) ^b
PCu2,5	28.0	0.58	110 000	48 200	1.89×10^8
CPCu2	0.37	6.10	1450	61	2.40×10^5
PZn2,5Cu	10.2	0.73	40 100	14 000	5.50×10^7
CPZn2Cu	0.35	6.15	1380	57	2.24×10^5
PCu3,5	105	0.36	413 000	292 000	1.15×10^9
CPCu3	1.15	4.16	4520	276	1.08×10^6

^a The control polymers **CPCu2** and **CPCu3** were prepared in the same manner as **PCu2,5** and **PCu3,5**, only the template **5** was substituted by formic acid. ^b $K_{\text{ix}}^{-1} = (k_{\text{cat}}/K_{\text{m}})/k_{\text{unecat}}$ (catalytic proficiency).¹⁸

as a porogen failed owing to the poor solubility of the Cu(II) complex of functional monomer and template in MeCN. The reason for the poor efficiencies of the catalysts prepared in a polar solvent like DMF and DMSO is a twofold one. First, the interaction among monomer, template, and metal ion is less pronounced compared to nonpolar solvents. Second, in these solvents somewhat different physical properties of the macroporous polymers are observed; thus the stability of the active sites with regard to shape and arrangement of functional groups is less pronounced. Both effects lead to less precisely imprinted active sites and therefore lower catalytic efficiency.

The highest catalytic enhancements were achieved using the imprinted polymer **PCu3,5** prepared with the newly designed monomer **3** (see Table 1). In this polymer two amidinium moieties were introduced in a certain proximity to one Cu(II) center in the imprinted cavity (see Scheme 4c, d). This imprinted polymer **PCu3,5** shows the strongest catalytic activity with a rate enhancement for $k_{\text{impr}}/k_{\text{soln}}$ of 98 200-fold for the hydrolysis of substrate **7**; in the case of substrate **8** a further rate enhancement to an extremely high value of 217 000-fold was observed.

As with natural enzymes the catalysis of the carbonate hydrolysis by imprinted polymers follows typical Michaelis–Menten kinetics (Figure 5). A plot of initial velocities of the reaction versus the substrate concentration shows at first an increase in the rate of reaction with increasing substrate, and the rate then levels off. At a higher substrate concentration, when all of the active sites are occupied, the rate remains constant which means it is zero order with respect to carbonate concentration (saturation kinetics). The turnover number k_{cat} and the Michaelis constant K_{m} can be calculated from the double reciprocal plots of the initial rate versus the substrate concentration (Lineweaver–Burke plot) or by fitting the Michaelis–Menten curve to a hyperbola using the program Origin 7.0. Strong turnover numbers have been observed for all imprinted polymers with a catalytic center of Cu(II). The k_{cat} is 2.86 min⁻¹ for hydrolysis of **7** by **PCu2,5** and 28.0 min⁻¹ for **8**; in the case of **PCu3,5** with two amidinium moieties in proximity to the Cu(II) center, a remarkable turnover number for the hydrolysis of **8** of $k_{\text{cat}} = 105 \text{ min}^{-1}$ was obtained (see Table 3).

$k_{\text{cat}}/k_{\text{unecat}}$ is usually used to express the catalytic activity of catalytic antibodies and natural enzymes. **PCu2,5** showed a $k_{\text{cat}}/k_{\text{unecat}}$ of 110 000 for the hydrolysis of **8**, a rather high value for a synthetic enzyme model. **PCu3,5** showed an even higher rate enhancement of 413 000-fold for the hydrolysis of **8**; it is by far the highest value reported until now for molecularly

(18) (a) Miller, B. G.; Wolfenden, R. *Annu. Rev. Biochem.* **2002**, *71*, 847–885. (b) Zhang, X.; Houk, K. N. *Acc. Chem. Res.* **2005**, *38*, 379–385.

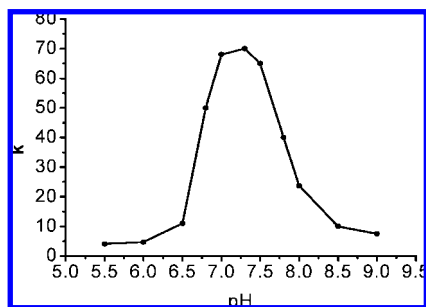


Figure 7. pH Profile of the Rate of Hydrolysis of **6** in Presence of 0.048 mM Active Sites of **PCu2,5**. Buffer solution/MeCN 1:1. Buffers used were pH 5.5–6.5 MES; pH 7.3–8.1 HEPES; pH 8.4–9.5 CHES. k (10^{-1} min^{-1}).

imprinted catalysts. The Michaelis constants K_m demonstrate a much better binding in the imprinted polymers compared to the control polymers (see Table 3). By combination of substrate recognition and catalysis the catalytic efficiency can be recognized. The imprinted polymers exhibit by far better catalytic efficiencies k_{cat}/K_m ($\text{min}^{-1} \text{ M}^{-1}$) compared to the control polymers; for example, enhancement factors of 1056 and 790 for the hydrolysis of **8** by **PCu3,5** and **PCu2,5** were observed in comparison to the controls **CPCu3** and **CPCu2**, respectively.

However, for the hydrolysis of **8** by **PZn2,5Cu** which was prepared by substitution of Zn(II) by Cu(II) from Zn(II)-imprinted polymer **PZn2,5**, this value is significantly lower (245). Obviously, the remarkable differences in the catalytic efficiency relate to the accuracy of the imprinting procedure. k_{cat}/K_m is an important measure for the efficiency of enzymes and enzyme analogues. In order to include in the assessment of enzymes the difference in the difficulty of the tasks that they perform, it is necessary to know the reaction rate under uncatalyzed conditions and relate the efficiency to this reaction rate. Thus $(k_{\text{cat}}/K_m)/k_{\text{uncat}}$ has been introduced by Wolfenden¹⁸ and called the catalytic proficiency K_{ix}^{-1} . The proficiency is formally the equilibrium constant for the formation of the complex between the transition state and the enzyme or enzyme model. It therefore reflects the hypothetical binding affinity of an enzyme for the transition state.¹⁸ Our new imprinted polymers were shown to possess very high K_{ix}^{-1} values (10^8 – 10^9 M^{-1}) in catalysis which are, as the efficiencies, significantly higher by 2 to 3 orders of magnitude compared to the nonimprinted control polymers (Table 3). These differences are remarkable since the control polymers also contain the same catalytically active functional groups. The comparison of K_{ix}^{-1} for imprinted polymers and the control polymers unambiguously demonstrates the stabilization of the transition state in the imprinted cavities. Interestingly, K_{ix}^{-1} is higher for **PCu3,5** compared to **PCu2,5** which means the transition state is more firmly bound though the imprinting factor is somewhat lower (50 instead of 80; see Table 2).

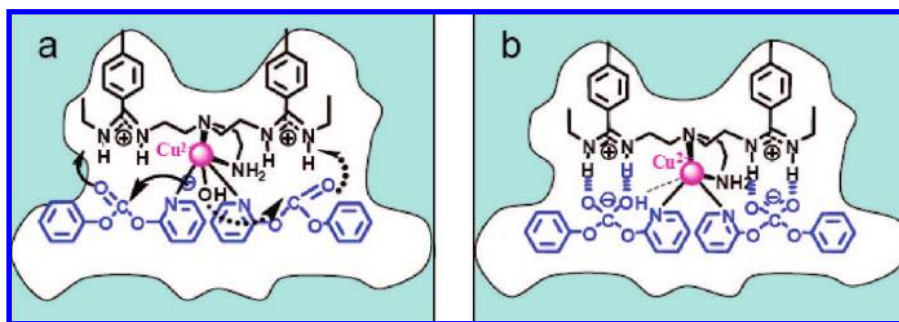
With regard to the mechanism of catalysis for these imprinted catalysts it is important that the active site of **PCu2,5** contains a copper *aqua hydroxy* form (see Scheme 4 b), which is the catalytically most active form.^{2e} This has been demonstrated in our case by measuring the pH profile for the carbonate hydrolysis in the presence of **PCu2,5** (see Figure 7). It shows a typical bell-shaped profile with an optimum at pH 7.2. The maximum rate is obtained when the *aqua hydroxy* form is at its highest level. Similar catalysts with Cu^{2+} and guanidinium ions for peptidase activity were investigated by Suh and co-

workers.^{2f} Their catalysts correspond to our nonimprinted control systems such as **CPCu2**.

A unique bifunctional catalysis (similar to that postulated by Breslow^{2d} for the enolization of ketones) proceeds in the imprinted polymers such as **PCu2,5** via a binding of the pyridyl ring of **7** or **8** to the copper ion and an activation of the carbonyl group by the protonated amidinium ion followed by the attack of the copper bound hydroxyl group to the carbonyl group. The reaction is further accelerated by the stronger binding of the tetrahedral transition state compared to the original substrate. The mechanism in the imprinted polymer **PCu3,5** is more complicated. Two amidinium moieties are oriented in a certain proximity to one Cu^{2+} center (see Scheme 6). The coordination of the copper ion is therefore quite different compared to **PCu2,5**. Whereas in the active site of **PCu2,5** (Scheme 4b) copper undergoes three coordinative bonds to amines, in **PCu3,5** there are only two coordinative bonds to amines; this influences the catalytic activity of the additional groups bound to copper like H_2O and OH^- . During binding of substrates, this becomes even more complicated since the active site can bind either one or two molecules of substrate. In the case of binding two molecules of substrate **7**, copper will be coordinated to four nitrogens, and in the case of one molecule of substrate **7**, copper will be coordinated by three nitrogens. Coordination of copper to the nitrogens of the amidines is not to be expected since there complexation is much lower as the potentiometric pH titrations also show. Usually catalysts like enzymes are used under subsaturation conditions, meaning that mixed mechanisms are to be expected with one or two substrates per active site. One possible route for the catalysis with the imprinted polymer **PCu3,5** proceeds via binding of two substrates in one cavity as shown in Scheme 6a and an activation of the carbonyl group by the protonated amidinium ion, followed by attack of the copper bound hydroxyl group. The reaction is further accelerated by the preferred binding of the tetrahedral transition state (Scheme 6b). It was shown that the carbonate hydrolysis can be competitively inhibited by adding the TSA template. The decrease in V_{max} and the effective inhibition constant (e.g., $K_i = 25 \mu\text{M}$, for the hydrolysis of **8** by **PCu2,5** and inhibited by template **5**) indicates that cavities with high affinity for TSA are responsible for rate enhancement (Scheme 6b). This is a further proof for the effect of the molecular imprinting.

By achieving a combination of a preferred binding of the transition state in the imprinted active sites and a proper orientation of the catalytic moieties, a high catalytic efficiency and proficiency of molecularly imprinted polymers have been obtained. Rate enhancements ($k_{\text{cat}}/k_{\text{uncat}} = 4.1 \times 10^5$) are even higher by more than 500-fold compared to catalytic antibodies for which $k_{\text{cat}}/k_{\text{uncat}} = 810$ has been reported for carbonate hydrolysis.¹⁹ The examples reported here are the first examples where the catalytic activity of molecularly imprinted polymers obviously surpasses the activity of the catalytic antibodies reported (generally the catalytic rate enhancements for catalytic antibodies is on the order of $k_{\text{cat}}/k_{\text{uncat}} = 10^2$ – 10^4).³ However, in natural enzymes $k_{\text{cat}}/k_{\text{uncat}}$ can go up much higher with values of 10^6 – 10^{20} . The catalytic proficiency K_{ix}^{-1} in our examples goes up to values of 10^8 – 10^9 M^{-1} . Compared to natural enzymes with 10^7 – 10^{23} M^{-1} our catalysts are approaching the less proficient enzymes.¹⁸ The catalytic efficiency for our catalysts ($k_{\text{cat}}/K_m = 3 \times 10^5 \text{ min}^{-1} \text{ M}^{-1}$) is lower compared to enzymes.

(19) Jacobs, J. W.; Schultz, P. G.; Sugawara, R.; Powell, M. J. *Am. Chem. Soc.* **1987**, *109*, 2174–2176.

Scheme 6. Schematic Representation of the Binding and Catalysis of Substrates in the Cavities of the Imprinted Polymer **PCu3,5**^a

^a (a) Substrate **7** bound in the cavity of the imprinted polymer catalyst **PCu3,5**. (b) Intermediate in the catalysis by imprinted polymer catalyst **PCu3,5** (in both cases with reactions of two substrates at the same time).

In the present enzyme model, the cavities of the molecularly imprinted polymers are designed toward a single TSA template. Therefore, the affinity induced by the TSA imprinting is used preferentially for TS stabilization. This is in contrast to natural enzymes which are evolved to recognize a series of structures that connect the substrate and the multistep transition states along the reaction pathway.²⁰ Furthermore, enzymes are evolved to have a flexible surface to stabilize not only the TS but also the intermediate states in a multistep reaction.^{1,20} In comparison, the cavities generated by molecular imprinting exhibit a more rigid structure owing to the use of a high degree of cross-linking agent in the polymerization process but still have some flexibility and swellability. The relatively slow mass transfer inside the molecularly imprinted polymers and the “polyclonality” (the active sites prepared by imprinting with one template do not all have exactly the same structure) of imprinted cavities are also obstacles for further improvement of the catalysis. Although this approach is intellectually promising, there still is a long way to go to design molecularly imprinted catalysts that can compete with naturally occurring enzymes with regard to their activity and selectivity.

4. Conclusion

New models for the enzyme carboxypeptidase A were prepared by molecular imprinting showing high catalytic efficiency. This was achieved by a combination of molecular imprinting using a stable transition state analogue as a template and the introduction of amidinium functions and a Cu²⁺ binding site in the active site in a predetermined orientation. These models show typical enzyme properties such as selectivity, Michaelis–Menten kinetics, competitive inhibition, and a bell-shaped curve of the pH rate profile. They represent the most

active catalysts prepared by the molecular imprinting strategy. The catalytic activity, the catalytic efficiency, and the catalytic proficiency are clearly surpassing those of the catalytic antibodies and approaching those of the natural enzymes. This strategy provides a promising tool to elucidate the role of transition state stabilization in enzyme catalysis and shows direct evidence supporting Pauling’s transition state stabilization theory. The study demonstrates that molecularly imprinted polymers offer an excellent possibility to mimic the active site of natural enzymes not only by mimicking the shape of the transition state but also for introducing suitable catalytically active groups into the active site in a predetermined orientation. It is also possible to introduce catalytic groupings that do not exist in nature and which cannot be introduced by biochemical methods.

From these results some important information to improve the catalytic efficiency of molecularly imprinted polymer catalysts can be summarized: First, the affinity of molecularly imprinted polymers for their related transition states should be high. Second, the orientation of the catalytic moieties with respect to the reactive groups of the substrates has to be optimized. The high efficiency and selectivity together with the strong chemical, mechanical, and thermal stability as well as the relatively simple preparation method give these catalysts a real advantage compared to catalytic antibodies and also provide a good alternative compared to natural enzymes.

Acknowledgment. This research was supported by Deutsche Forschungsgemeinschaft and Fonds der Chemischen Industrie and by the National Natural Science Foundation of China (20534030, 20725415), the 111 project (B06009). J.-q.L. acknowledges a fellowship from the Alexander von Humboldt Foundation. Helpful discussions with Prof. Dr. W. Kläui, Institute of Inorganic Chemistry of the Heinrich Heine University, are greatly acknowledged.

(20) Fersht, A. *Structure and Mechanism in Protein Science: A Guide to Enzyme Catalysis and Protein Folding*, 3rd ed.; Freeman, W. H. and Company: New York, 2000.